# Enhanced performance of GaN-based light-emitting diodes with InGaN/GaN superlattice barriers*

Cai Jin-Xin(蔡金鑫), Sun Hui-Qing(孙慧卿)†, Zheng Huan(郑 欢), Zhang Pan-Jun(张盼君), and Guo Zhi-You(郭志友)

*Laboratory of Nanophotonic Functional Materials and Devices, Institute of Opto-Electronic Materials and Technology, South China Normal University, Guangzhou* 510631, *China*

(Received 24 July 2013; revised manuscript received 9 November 2013; published online 18 March 2014)

GaN-based multiple quantum well light-emitting diodes (LEDs) with conventional and superlattice barriers have been investigated numerically. Simulation results demonstrate using InGaN/GaN superlattices as barriers can effectively enhance performances of the GaN-Based LEDs, mainly owing to the improvement of hole injection and transport among the MQW active region. Meanwhile, the improved electron capture decreases the electron leakage and alleviates the efficiency droop. The weak polarization field induced by the superlattice structure strengthens the intensity of the emission spectrum and leads to a blue-shift relative to the conventional one.

**Keywords:** superlattice barrier, numerical simulation, hole injection, GaN-based LED

**PACS:** 85.60.Jb, 78.60.Fi, 87.15.A−, 73.61.Ey **DOI:** 10.1088/1674-1056/23/5/058502

## 1. Introduction

In recent years, blue InGaN light-emitting diodes (LEDs) spread in optoelectronic products, especially in general illumination, to replace conventional lamps, due to their high potential efficiencies.[1–3] However, InGaN LEDs still suffer from a serious decrease of the power efficiency as the injection current increases, mainly because of electron leakage,[4,5] inefficient hole injection,[6] carrier delocalization,[7] and auger recombination rate.[8] Different kinds of electron blocking layers (EBLs), such as p-AlInN EBL,[9] AlGaN/GaN superlattice EBL,[10] and chirped AlGaN MQBs,[11] are utilized to suppress the electrons to escape from the last QW, where the maximum electrons accumulate and the mainly radiative recombination happens in traditional GaN-based LEDs. However, these methods can only improve hole injection without transport in an active region. Hence, how to enhance the symmetrized carrier distribution and the uniform radiative recombination implies good promise for the development of the LEDs. Various barriers have been proposed to improve hole injection and reduce the polarization effect between the well and the barrier induced by the lattice mismatch, such as InGaN barriers,[12] AlInGaN barriers,[13] tailored Si-doping barriers,[14] and so on. Liu *et al.*[15] proposed that a decrease in the thickness or the height of the potential barrier increases hole injection into the MQWs located near the n-GaN layer in InGaN LEDs. However, the shallower band gap resulted in the losing of carriers confined capability as well. Zhu *et al.*[14] demonstrated an example of uniform carrier distribution and radiative recombination by adjusting the doping profile in different barriers, which minimized electron leakage and improved efficiency. Barriers with three 5-nm-thick nitride layers were adopted to reduce polarization without decreasing quantum potential height, which also improved hole injection and transport due to the appropriately modified energy band diagrams.[16,17] Based on the above, methods to improve hole injection and transport are still under intensive investigation.

As quantum tunneling can allow the current to flow through high barriers properly, and periodic structures also support miniband tunneling at some carrier energies (Esaki–Tsu model),[18] many superlattice structures are adopted in the epitaxial wafer to replace the traditional layers.[10,19,20] The introduction of the superlattice barriers[18] may be a good method to overcome the above problems. In previous work, the performances of the LED with AlGaN/InGaN superlattice barriers have been discussed by simulation and experiment,[21–23] but the problem of band gap decreasing appears when the InGaN layer of the barrier contacts to the InGaN well layer, and the Al component increases the strain in the period active layers, which strengthens the formation of the V-pits and deteriorates the interface crystal quality. Therefore, the performances of the LED structure with InGaN/GaN superlattice barriers are investigated in this work.

## 2. Structure and parameters

The GaN-based LEDs are grown on a *c*-plane sapphire substrate. From the bottom to the top, the traditional LED structure, labeled as LED-A, consists of a 100-μm-thick sapphire substrate, a 1.5-μm-thick GaN buffer layer, a 3-μm-thick n-type GaN (n-doping: $5 \times 10^{18}$ cm$^{-3}$), six pairs of undoped InGaN (3 nm)/GaN (9 nm) MQWs active region, a 20-nm-thick p-type $Al_{0.15}Ga_{0.85}N$ (p-doping: $1 \times 10^{18}$ cm$^{-3}$) EBL, and a 150-nm-thick p-type GaN (p-doping: $1 \times 10^{18}$ cm$^{-3}$).

*Project supported by the National Natural Science Foundation of China (Grant No. 60877069) and the Science and Technology Key Program of Guangdong Province, China (Grant Nos. 2011A081301004 and 2012A080304006).

†Corresponding author. E-mail: sunhq@scnu.edu.cn

© 2014 Chinese Physical Society and IOP Publishing Ltd 

Another structure, labeled as LED-B, has the last GaN barrier replaced by the $In_{0.05}Ga_{0.95}N$/ GaN superlattice barrier, which is similar to the structure investigated by Liu *et al.*[23] For the third structure, labeled as LED-C, we replace all the barriers by $In_{0.05}Ga_{0.95}N$/GaN superlattice barriers. The device geometry is designed into a rectangular shape of $300 \times 300$ μm$^2$. The structures of the three LEDs are shown in Fig. 1. The electrical and optical performances are investigated by using APSYS[24] modeling software. In the simulation, the operating temperature is estimated to be 300 K. The auger recombination coefficient, Shockley–Read–Hall (SRH) lifetime, and background loss in the QWs are assumed to be $1 \times 10^{-30}$ cm$^6$/s, 100 ns, and 2000 cm$^{-1}$, respectively.[11] The InGaN and AlGaN bandgap energies are expressed by the formula proposed by Vurgaftman *et al.*,[25] where the bandgap energies of InN, AlN, and GaN are 0.78 eV, 6.25 eV, and 3.51 eV, and the bowing parameters of InGaN and AlGaN are 1.43 eV and 1.0 eV, respectively.[26] The interface charge densities induced by the fixed defects are calculated assuming 30% compensation, according to the formulas developed by Fiorentini *et al.*[27] Other material parameters used in the simulation can be found in Ref. [28].

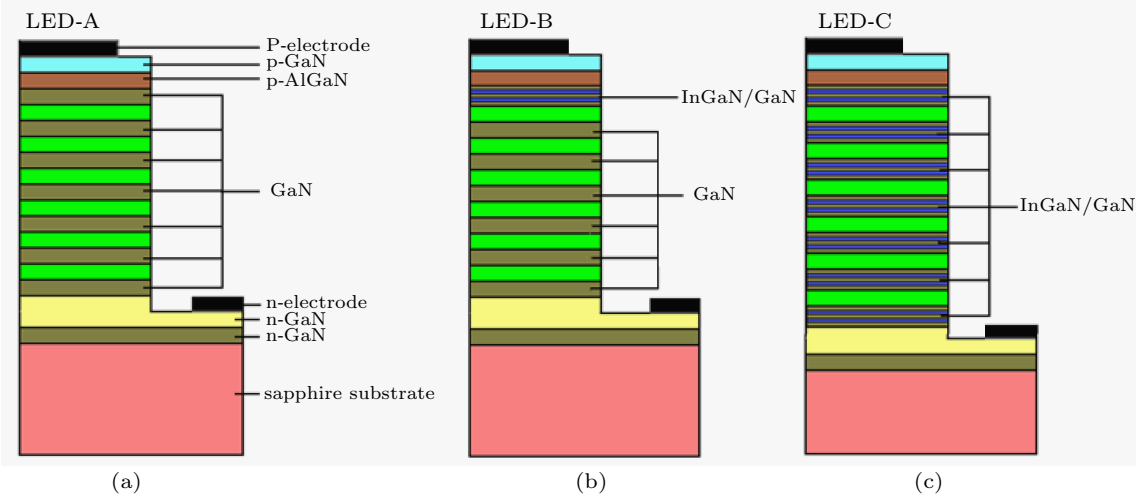



**Fig. 1.** Schematic diagrams of the three LEDs. (a) LED-A, (b) LED-B, (c) LED-C.

## 3. Results and discussion

Figure 2 shows the current versus voltage (*I*–*V*), the light output power (*L*–*I*), and the internal quantum efficiency (IQE) curves of the three LEDs. The values of the light output power of the three LEDs at 300 A/cm$^2$ are provided in Table 1. From Fig. 2(a), we can see that the *I*–*V* cure of the LED-A is very close to LED-B, but the LED-C has a higher forward voltage indicating the carrier transport in the superlattice barrier is different from the conventional barrier, which will be shown later. It is found that LED-A always has the lowest light output power, and when the forward current density is 300 A/cm$^2$, the LED-B has a 43.4% increase in the light output power contrasts to LED-A, while LED-C has 59.2%. Figure 2(b) shows the internal quantum efficiency and illustrates that a sharp peak appears in LED-A at a small current density below 10 A/cm$^2$; but the efficiency rapidly decreases 43.8% at the larger current density of 300 A/cm$^2$. On the contrary, LED-B and LED-C exhibit an efficiency droop of 27.9% and 23% under the same conditions. Thus, LEDs with InGaN/GaN superlattice barriers show better performances than the conventional one at the large forward bias.

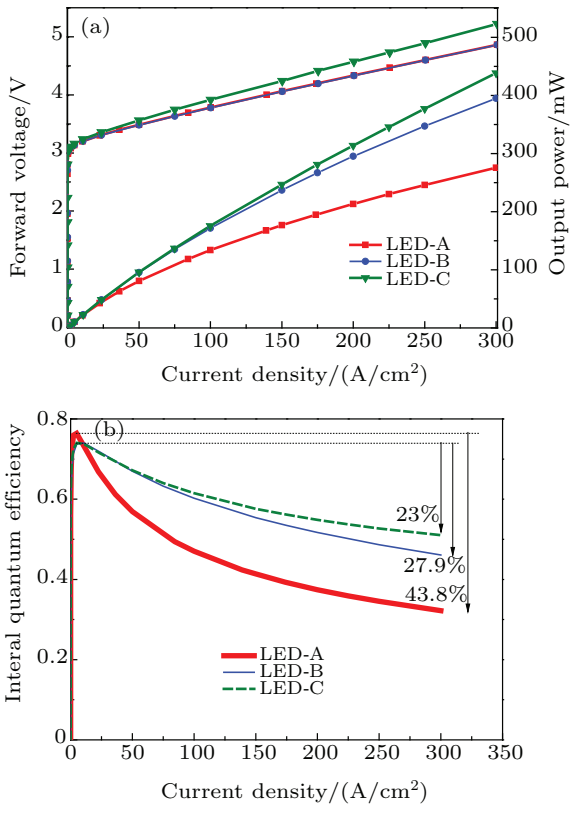



**Fig. 2.** Simulated *I*–*V* and *L*–*I* (a), and IQE (b) curves of the LEDs with conventional and InGaN/GaN superlattice barriers.

**Table 1.** Light output power of the three LEDs at 300 A/cm$^2$.

| Group | Light output power/mW |
|---|---|
| LED-A | 275.5 |
| LED-B | 395.1 |
| LED-C | 438.6 |

Figure 3 shows the calculated band profiles (Figs. 3(a)–3(c)) and carriers distributions (Figs. 3(d)–3(f)) of the three LEDs with different barrier structures at the current density of 200 A/cm$^2$. Comparing LED-B with LED-A, we can see that the introduction of InGaN/GaN superlattice barriers can dramatically improve the negative downward band-bending of the last barrier, owing to the large spontaneous and piezoelectric polarization originating from the lattice mismatch between the EBL and the last barrier. This not only improves the effective potential barrier height for electrons in the conduction band but also lowers it for holes in the valance band of the EBL. Therefore, the holes are easy to inject into the last QW while the electrons are confined in the same region, which leads to the increase of the radiative recombination. This result agrees with that in Ref. [22]. It is also found that a potential "valley" below the quasi-Feimi level appears in the conductive band in the last barrier of the LED-B.[29] The "valley" is considered different from the one appearing between the last barrier and the EBL in LED-A, which separates the carriers, prolongs the lifetime of the electrons, and hence increases the auger recombination and electron leakage. As holes also accumulate in the InGaN layers of the superlattice barrier, these electrons may be captured by holes, resulting in the suppression of efficiency droop. From Fig. 3(c), we can see LED-C not only shows all the superior performances of LED-B but also gets other characters in the active region. Compared with LED-B, LED-C has an 8-meV lower effective potential barrier height for electrons but 11-meV lower for holes, which is attributed to the miniband tunneling model of the superlattice. It implies that the transport of the holes is enhanced, which is confirmed in Fig. 3(f).

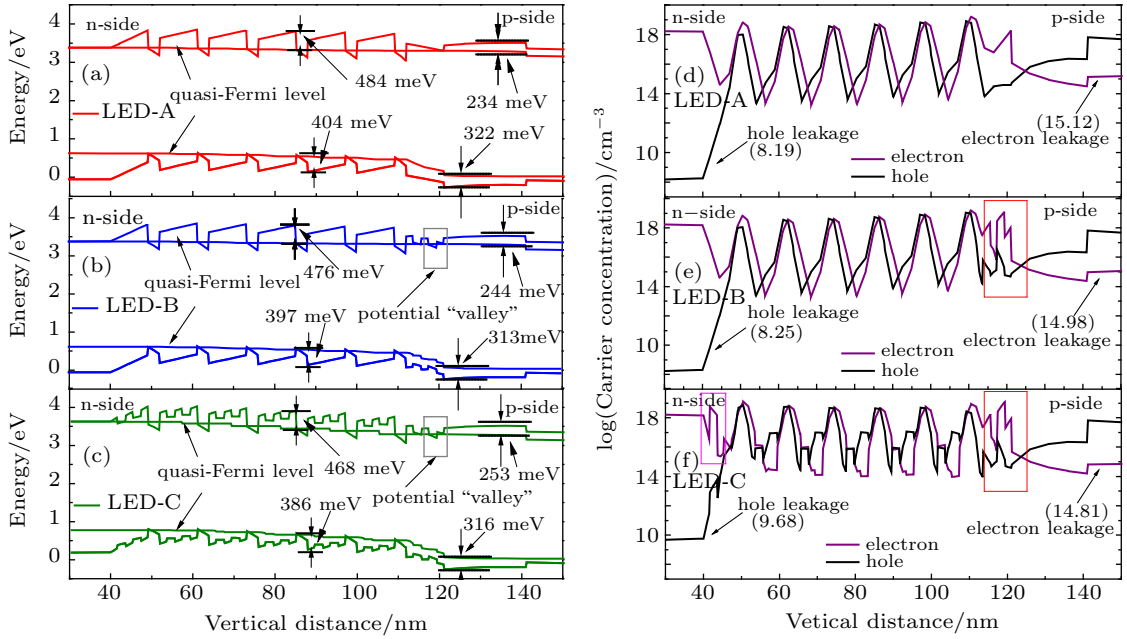



**Fig. 3.** Band diagrams ((a)–(c)) and carrier distributions ((d)–(f)) of the LEDs with the conventional and InGaN/GaN superlattice barriers at 200 A/cm$^2$.

Carefully analysing Figs. 3(d)–3(f), we can see the overlap of electron hole distribution in QWs is significantly increased in LED-C, owing to more uniform hole distributions and weaker polarization in the MQWs, and the last QW will not be the most contributing QW to optical emission, which is different from LED-A and LED-B. It is found that the electron leakage is also deduced as discussed above. Although the hole leakage appearing in the LED-C is many times larger than the other two LEDs, it still can be ignored due to its small value and few effects. Therefore, the efficiency droop is suppressed effectively. Moreover, it is found that the first barrier induces an electron accumulation point, which also acts as a current spread layer.[21]

Taking the energy-band and carrier distribution diagrams into account, we can see the potential height and carrier concentration is diverse in different InGaN layers of the InGaN/GaN superlattice barriers. Parameters, such as In composition, period of InGaN/GaN layer, should be further optimized to obtain the superior performances.

Figure 4 shows the spontaneous emission spectra of the three LEDs at the current densities of 50 A/cm$^2$ and 200 A/cm$^2$, respectively. It is found that the intensities of the LED with InGaN/GaN superlattice barriers are always larger than the conventional one, which is more obvious at large forward bias. Moreover, we can see the intensities of LED-B and LED-C are very close when the current density is

only 50 A/cm$^2$, but the LED-C has a significant advantage at 200 A/cm$^2$. It is attributed to the enhancement of hole transport. When the last barrier is replaced by the InGaN/GaN superlattice, the improvment of the hole injection increases the hole concentration in the MQWs region. As most of the radiative recombination of LED-B happens in the last QW, the limited hole accumulation can effectively enhance the spontaneous emission rate at low current density. However, because the hole has a relatively high effective mass and a very low mobility making hole transport in the active region difficult, the advantages of LED-B are limited at large forward bias. However, LED-C would not suffer from this problem. The InGaN/GaN superlattice barrier structure droops and the effective potential barrier height largely improves the hole transport, resulting in hole density becomeing uniform and most QWs contribute to the radiative recombination. Thus, the spontaneous emission spectrum of LED-C shows the highest intensity in the three LED simples. The other important phenomenon is the blue-shift appearing in the LED-B and LED-C. Due to the spectral blue-shift, it is determined by the competition between a spectral read-shifting mechanism of the piezoelectricity-induced quantum confined Stark effect (PQCSE) and other causes; it is found that the weak polarization field induced by the superlattice structure results in this blue-shift, which also agrees with the band diagram shown in Figs. 3(a)–3(c).

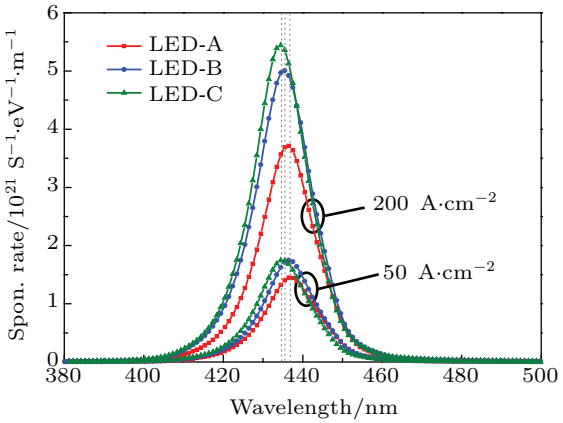



**Fig. 4.** Spontaneous emission spectra of the LEDs with the conventional and InGaN/GaN superlattice barriers at 50 A/cm$^2$ and 200 A/cm$^2$.

## 4. Conclusions

In summary, the LEDs with InGaN/GaN superlattice barriers are proposed and simulated in this work. When the last barrier of a conventional LED is replaced by the InGaN/GaN superlattice barrier, the hole injection is dramatically increased without decreasing the electron confinement, and performances are improved as well. When all the barriers adopt InGaN/GaN superlattice barriers, the amelioration of hole injection and transport results in more symmetrized carrier transport and more even carrier distributions among the QWs. The efficiency and light output power are further improved. The InGaN/GaN superlattice barriers can suppress the strain in the interface. We also demonstrated the spontaneous emission spectra of LEDs with different barriers. The stronger intensity implies that the LEDs with superlattice barriers have better optical performance.

## References

[1] Zhang J M, Zou D S, Xu C, Zou Y X, Liang T, Da X L and Shen G D 2007 *Chin. Phys.* **16** 1135
[2] Cao D X, Guo Z Y, Liang F B, Yang X D and Huang H Y 2012 *Acta Phys. Sin.* **61** 138502 (in Chinese)
[3] Du X Z, Lu H, Chen D J, Xiu X Q, Zhang R and Zheng Y D 2010 *Chin. Phys. Lett.* **27** 088105
[4] Schubert M F, Xu J, Kim J K, Schubert E F, Kim M H, Yoon S, Lee S M, Sone C, Sakong T and Park Y 2008 *Appl. Phys. Lett.* **93** 041102
[5] Mao A, Cho J, Schubert E F, Son J K, Sone C, Ha W J, Hwang S and Kim J K 2012 *Electron. Mater. Lett.* **8** 1
[6] Chang Y A, Chang J Y, Kuo Y T and Kuo Y K 2012 *Appl. Phys. Lett.* **100** 251102
[7] Vaxenburg R, Lifshitz E and Efros Al L 2013 *Appl. Phys. Lett.* **102** 031120
[8] Monemar B and Sernelius B E 2007 *Appl. Phys. Lett.* **91** 181103
[9] Lu T P, Li S T, Zhang K, Liu C, Xiao G W, Zhou Y G, Zheng S W, Yin Y A, Wu L J, Wang H L and Yang X D 2011 *Chin. Phys. B* **20** 098503
[10] Gong C C, Fan G H, Zhang Y Y, Xu Y Q, Liu X P, Zheng S W, Yao G R and Zhou D T 2012 *Chin. Phys. B* **21** 068505
[11] Xia C S, Li Z M S, Li Z Q and Sheng Y 2013 *Appl. Phys. Lett.* **102** 013507
[12] Wang L, Wang J X, Zhao W, Zou X and Luo Y 2010 *Chin. Phys. B* **19** 076803
[13] Fu Y K, Jiang R H, Lu Y H, Chen B C, Xuan R, Fang Y H, Lin C F, Su Y K and Chen J F 2011 *Appl. Phys. Lett.* **98** 121115
[14] Zhu D, Noemaun A N, Schubert M F, Cho J, Schubert E F, Crawford M H and Koleske D D 2010 *Appl. Phys. Lett.* **96** 121110
[15] Liu J P, Ryou J H, Dupuis R D, Han J, Shen G D and Wang H B 2008 *Appl. Phys. Lett.* **93** 021102
[16] Kuo Y K, Wang T H and Chang J Y 2012 *Appl. Phys. Lett.* **100** 031112
[17] Tong J H, Li S T, Lu T P, Liu C, Wang H L, Wu L J, Zhao B J, Wang X F and Chen X 2012 *Chin. Phys. B* **21** 118502
[18] Wacker A 2002 *Phys. Rep.* **357** 1
[19] Xiong J Y, Zhao F, Fan G H, Xu Y Q, Liu X P, Song J J, Ding B B, Zhang T and Zheng S W 2013 *Chin. Phys. B* **22** 118504
[20] Noh Y K, Kim M D and Oh J E 2011 *J. Appl. Phys.* **110** 123108
[21] Jia C Y, Yu T Y, Lu H M, Zhong C T, Sun Y J, Tong Y Z and Zhang G Y 2013 *Opt. Express.* **21** 7
[22] Luo D F, Chen C P and Peng J 2013 *Chin. Phys. Lett.* **30** 038504
[23] Liu X P, Fan G H, Zheng S W, Gong C C, Lu T P, Zhang Y Y, Xu Y Q and Zhang T 2013 *Sci. China Tech. Sci.* **56** 98
[24] Crosslight Software Inc. Burnaby, Canada
[25] Vurgaftman I, Meyer J R and Ram-Mohan L R 2001 *J. Appl. Phys.* **89** 5815
[26] Wu J 2009 *J. Appl. Phys.* **106** 011101
[27] Fiorentini V, Bernardini F and Ambacher O 2002 *Appl. Phys. Lett.* **80** 1204
[28] Piprek J and Li Z M S 2013 *Appl. Phys. Lett.* **102** 131103
[29] Liu Z Q, Ma J, Yi X Y, Guo E Q, Wang L C, Wang J X 2012 *Appl. Phys. Lett.* **101** 261106